



Underpotential Deposition of Silver on Pt(111):
Part I. Concentration Dependence

ONR

J.F. Rodríguez, D.L. Taylor and H.D. Abruña*

Department of Chemistry

Baker Laboratory

Cornell University

Ithaca, New York 14853-1301

1990

DTIC
ELECTE
JUN 06 1991
S D D

ABSTRACT

We report on the concentration dependence of the underpotential deposition of silver on well-defined Pt(111) electrodes. Electrochemical as well as ultra high vacuum surface techniques have been employed. We have found that when the silver ion concentration is 1.00 mM the electrodeposition is via adsorption in a well-defined manner, whereas at a concentration of 0.005 mM the mechanism involves three dimensional nucleation and island formation. In addition, two monolayers of silver are deposited at underpotentials but the stability of the second layer is a strong function of the silver ion concentration in solution. When the silver ion concentration is 1.00 mM, rinsing the electrode (with supporting electrolyte containing no silver in solution) at controlled potential results in essentially complete removal of the second layer of silver. However, when the deposition is from a solution containing silver at a concentration of 0.10 mM, the layer is stable to the same rinsing procedure.

DISTRIBUTION STATEMENT A

Approved for public release
Distribution Unlimited

91-00551



91 5 24 078

INTRODUCTION

The process of under potential deposition (UPD) of metals on foreign metal substrates has been studied with a wide variety of electrochemical and spectroscopic methods during the past two decades [1-14]. In particular, the electrodeposition of silver on platinum has received a great deal of attention [1-12]. In the early 1970's, Tindall and Bruckenstein [1] studied this system using a rotating-disk electrode and found that two UPD layers were deposited on the surface prior to bulk deposition. Cadle and Bruckenstein [2] then showed that Ag inhibited the adsorption of hydrogen blocking preferentially the weakly adsorbed sites. Using the twin electrode thin-layer technique, Stucki [3] concluded that after the deposition of two monolayers the Pt electrode acquire the properties of a bulk Ag electrode. Using X ray photoelectron spectroscopy, Hammond and Winograd [4] determined that the electrosorption of a monolayer of Ag on Pt was basically one.

Hubbard et. al. [5] showed specific surface structure formation at different stages of the electrodeposition process when Ag was deposited on an iodine pretreated Pt(111) surface. They also conclusively demonstrated the deposition of the second layer of silver by the appearance of an additional voltammetric peak prior to bulk deposition. The electrodeposition of Ag on a bare clean Pt(111) electrode was first reported by El Omar et. al. [6]. They also observed the deposition of the second layer, but no surface structures were presented in that study. Using Angular Distribution Auger Microscopy, Frank et. al. [7] concluded that the deposition of Ag was commensurate with the Pt(111) surface, although such structural assignments have generated a great deal of controversy.

Arvia et. al. [8] proposed that the deposition of silver on polycrystalline Pt was via a 2-D nucleation growth process and that alloying was evident under certain conditions. Further claims for alloy formation in polycrystalline Pt were presented by Alonzo and Scharifker [9]. Arvia et. al. [10] extended their studies to polyfaceted

and electrochemically faceted Pt(100) electrodes, but this time their findings were consistent with an adsorption-desorption-nucleation and growth mechanism. Alloy formation on these oriented surfaces was not evident. However, Aberdam et al. [11] observed surface alloying on a well defined Pt(100) electrode using Auger electron spectroscopy in the angle of incidence dependent mode. Soriaga et. al. have [12] suggested a surface reconstruction towards island formation of Ag at low coverages when negative potentials were applied to polycrystalline Pt surface in the presence of adsorbed iodine.

Although much work has been accumulated on this system, there is no comprehensive study on the mechanism of Ag electrodeposition as a function of concentration using well defined Pt surfaces. It has been tacitly assumed that the mechanism is the same at different concentrations because of the strong interactions between UPD Ag and Pt surfaces. However, one needs to consider that the mass transport to the electrode surface will not be the same and the mechanism of deposition may be different. It may also be possible that at different concentrations, surface structures of different stability may form. Furthermore, there may be a coupling and/or competition of (between) kinetic and thermodynamic aspects that may ultimately dictate the surface structure.

In this study, we coupled electrochemical methods with electron spectroscopic and diffraction techniques to study the mechanism of Ag as a function of its solution concentration, on a well-defined Pt(111) surface. We have found that for silver concentrations at or beyond 1.00 mM the electrodeposition is via adsorption in a well-defined manner, whereas at low concentrations (e.g. 0.005 mM) the mechanism involves three dimensional nucleation and island formation. We have also determined that rinsing the surface, with supporting electrolyte, after the deposition of the second layer from a 1.00 mM Ag⁺ solution removed most of the second layer. When the silver concentration was lowered to 0.10 mM and the

aforementioned experiment was repeated the second layer remained on the surface, suggesting much stronger interactions between the second and the first layer of Ag.

Accession For	
NTIS CRA&I	<input checked="" type="checkbox"/>
DTIC TAB	<input type="checkbox"/>
Unannounced	<input type="checkbox"/>
Justification	
By	
Distribution	
Availability Codes	
Dist	Avail & or Special
A-1	



EXPERIMENTAL

Solutions

All solutions were prepared with pyrolytically distilled water (PDW) [15]. Water from a Millipore-milli Q system was distilled through a heated Pt gauze (700°C) to remove traces of organic species. 0.10 M aqueous sulfuric acid (ULTREX, J.T. Baker) was used as the supporting electrolyte. Silver solutions of 1.00 mM, 0.10 mM, and 0.005 mM were prepared by dissolving Ag₂SO₄ (Aldrich Chem. Co., 99.999%) in the supporting electrolyte.

Pt(111) single crystals

Pt(111) single crystal disk electrodes of about 1 cm in diameter (ca. 3 mm thick) were obtained from the Materials Preparation Facility at Cornell University. They were grown from the melt, and the two faces were oriented and cut in the 111 direction. Chemical and metallographic polishing were performed until a finished mirror surface was obtained on both faces of the disk. The crystals were supported by two 0.050" platinum wires spot-welded to the side of the crystals. Prior to any experiments the crystals were immersed in hot nitric acid for 10 minutes.

For the ultra-high vacuum (UHV) experiments a thermocouple was also spot-welded to the edge of the crystal to monitor the annealing temperature. In these experiments, the crystal was cleaned by several cycles of heating to 800°C in 10⁻⁶ torr of oxygen for twenty minutes and ion bombardment (5 μA, 10⁻⁵ torr Ar) for ten minutes. Prior to the surface characterization, the sample was annealed to 825°C. Auger electron spectroscopy (AES) and low energy electron diffraction (LEED) were utilized to assure cleanliness and long range order of the surface as shown in Figure 1.

For the non UHV experiments the crystal was treated using Clavier's method [16], i.e., heated to approximately 1000°C in a gas/oxygen flame for three minutes and cooled in the vapor of the supporting electrolyte for one minute. The crystal was then quenched in the same solution. The waiting period for quenching was necessary to avoid surface stress on the single crystal [17]. Surface cleanliness was determined by cyclic voltammetry in 0.10 M H₂SO₄, showing the characteristic "butterfly" shape (Figure 2).

UHV chamber

An all stainless-steel ultra-high vacuum (UHV) chamber which couples instrumentation for surface characterization and electrochemistry was used in some of the experiments. The UHV apparatus (Figure 3) consisted of two different chambers: (i) The main chamber which contains low energy electron diffraction (LEED) optics, a cylindrical mirror analyzer for Auger electron spectroscopy (AES), an ion gun, and a quadrupole mass spectrometer (INFICON). The system was interfaced to an Apple Macintosh SE computer through a MacADIOS (GW Instruments) data acquisition unit; and (ii) An ante-chamber where all the electrochemical experiments were performed. This chamber was isolated from the main chamber through a gate-valve to avoid introduction of gases in the latter, when the electrochemical experiments were performed. This configuration also allowed the removal of water from the walls of the ante-chamber while the sample was maintained clean in the main chamber.

Transfer of the sample from the main to the ante-chamber was achieved via a magnetic horizontal manipulator using a bayonet-type holder. The gate-valve was closed after the sample was mounted in the ante-chamber, and ultra-high pure argon was purged through a hydrocarbon and an oxygen trap columns prior to the introduction to the ante-chamber. The electrochemistry was performed in a two

compartment glass cell separated by an ultra-fine frit. The reference electrode was Ag/AgCl(1M NaCl) and the counter electrode was a platinum foil located in the same compartment as the working electrode. *Only one face* of the single crystal was exposed to solution using the dipping technique. Special care was taken to avoid contributions from the supported platinum wires and the thermocouple (vide-supra) in the electrochemical response. The characteristic voltammetry for a clean well-ordered surface is shown in Figure 4. After being transferred back to the main chamber, the surface was characterized with AES and LEED. AES showed signals related to the metal and the supporting electrolyte (S and O) and the LEED pattern was (1X1) with slightly broader spots (Figure 5). No surface reconstruction was evident when the sample was exposed to the sulfate species. The voltammetry after this surface characterization step showed again the same response.

Electrochemical cell for non UHV experiments

Electrochemical experiments outside the UHV chamber were performed in a two compartment glass cell separated by an ultra-fine glass frit as shown in Figure 6. The compartments had 24/40 joints to assure a close system. A Ag/AgCl (1M NaCl) reference electrode was located in one of the compartments in combination with a platinum wire used as the auxiliary electrode. The Pt(111) working electrode was positioned in the other compartment exposing only one face to the solution. Pre-purified nitrogen was continuously introduced into the cell through one of three Luer joints to avoid oxygen contamination. Another Luer joint opening was used to vent the nitrogen, while the other was utilized to introduce solutions into the cell from bubblers which were continuously degassed with nitrogen. The solution was removed from the cell by aspiration from a lower Luer joint.

The rinsing experiments were performed as follows: (i) the electrode potential was swept at 2.0 mV/sec from 0.85V to a pre-determined value, (ii) the solution was

supporting electrolyte three times at the same potential, at more negative values or at the rest-potential, (iv) the electrode potential was swept in the positive direction to determine the amount of silver retained on the surface.

RESULTS AND DISCUSSION

Figure 7 shows the electrodeposition of Ag^+ from a 1.00 mM solution on two Pt(111) surfaces that were pre-treated differently. In Figure 7a, the surface was cleaned and characterized in the UHV chamber, whereas the electrode in Figure 7b was annealed in an oxygen-gas flame. The potential in both experiments was initially scanned in the negative direction at 2.0 mV/s starting from +0.85V. This potential was chosen because Ag^+ spontaneously adsorbs on Pt [18] and we wanted to start the deposition with as little Ag on the surface as possible, but also did not want to disrupt the long range order of the Pt(111) surface. It has been reported that in this potential region the formation of oxides on the Pt(111) surface is insignificant [16]. Furthermore, a scan from this potential in pure supporting electrolyte showed no peaks related to the reduction of surface oxides (Figure 8), and several scans in this potential region did not alter the voltammetric response. It is only when very positive potentials, e.g. +1.20V, are applied that the Pt(111) surface reconstructs [17, 19]. The deposition of Ag from a 1.00 mM solution onto a clean Pt(111) surface can be divided into four steps; (i) deposition of 1.30 ± 0.09 monolayers between +0.85V and +0.69V (Peak 1), (ii) deposition of 0.22 ± 0.03 monolayers in the potential region of +0.69V to +0.45V, (iii) a sharp peak (Peak 3) between +0.45V and +0.36V, which accounts for 0.81 ± 0.09 monolayers, and finally (iv) deposition of bulk Ag at potentials below +0.36V. The amount of Ag deposited in the various regions was determined from coulometric data as reported in Table 1.

All LEED patterns obtained with this system at different potentials showed a (1X1) pattern, but with broader spots and higher background intensity suggesting a commensurate and ordered deposition (Figure 9). Similar results have been obtained with vapor deposition where a Stranski-Krastanov growth mechanism was deduced [20, 21]. In this mechanism the first layer is deposited in an ordered

form and the second layer follows with three dimensional nucleation and the formation of islands.

When the potential is reversed (i.e. anodic sweep) to remove the deposited Ag from the Pt(111) surface, a peak corresponding to the dissolution of the second layer is observed (Peak 4). It is interesting to note that if the potential is reversed again towards the cathodic direction at +0.60V (prior to the stripping of the first monolayer) the deposition of the second layer takes place at more positive potentials and the peak is narrower than in the previous scan. This may involve a rearrangement of the second monolayer during its completion in such a way that the interactions with the first layer are stronger during the second cycle. Stripping of the first layer is achieved in the potential range of +0.70 to +0.92V. The total amount of Ag removed from the Pt(111) surface is the same as that deposited, evidence that no other process other than the deposition and stripping of Ag is taking place (Table 1). In addition, AES data showed minimal amounts of Ag with some oxygen and sulfur from the supporting electrolyte at +0.92V (Figure 10). Furthermore, LEED data showed a (1X1) pattern. Thus, the removal of Ag at +0.92V does not disrupt the long range order of the Pt(111) electrode surface although some electrolyte appears to be present on the surface. It can also be noticed that the removal of this first monolayer consists of a shoulder around +0.78V and the main peak at around +0.82V. This shoulder is associated with the stripping of Ag from the region of peak 2, whereas the main peak (peak 5) is related to the removal of Ag deposited under peak 1. It is also noteworthy that the deposition of Ag on the Pt(111) is the same for both pre-treatments of the surface, showing that both surfaces have the same long range order prior to electrodeposition.

Figure 11 shows the deposition from a 0.10 mM Ag⁺ solution onto a Pt(111) surface. The potential was again started at +0.85V using a scan rate of 2.0 mV/s. The features of the deposition are similar to those in 1.00 mM Ag⁺, in which four

distinct regions are present. The charge under these regions is similar to that in the previous case as shown in Table 1. The potential shift of peaks 1 and 2 with silver concentration does not follow the reversible behavior of 60 mV/decade as expected from the Nernst equation if the electrosorption valency and the activity for the deposited monolayer were one (Table 2). However, the deposition of the second layer (Peak 3) does follow such behavior, although the deposition from 0.10 mM solution is more sluggish than at 1.00 mM Ag^+ , and the separation from bulk deposition is not as well defined. This difference may be attributed to kinetic complications due to the lowering of the Ag^+ concentration. We demonstrated this point by slowing the potential scan rate to 0.5 mV/s. At this slow scan rate, the peak becomes sharper and the separation from the bulk region is better defined, as shown in Figure 12. In addition, the charge under the peak becomes similar to the one obtained at higher concentrations.

Stripping of the bulk Ag and the second layer are accomplished when the potential scan was reversed in the positive direction. Only the stripping peak of the bulk Ag follows the reversible behavior of 60 mV/decade change in silver concentration. The shift of the stripping peak of the second layer was only 29 mV/decade. The potential scan was again reversed at +0.60V, prior to the removal of the first layer, and in this case there was no positive shift in the wave as it was for 1.00 mM Ag^+ solution. Therefore, it seems that there is no rearrangement of the second layer at this concentration. It can be also noticed that although the charge under the stripping peak for the second layer in 0.10 mM is the same as in 1.00 mM Ag^+ (Table 1); in the former case the peak is broader suggesting that removal of the second layer is from multiple energy sites of the first layer or that lateral interactions between Ag species are significant at this concentration. Stripping of the first layer is similar to that in 1.00 mM Ag^+ , in which the main peak is accompanied by a shoulder at a lower potential. However, when the scan rate is lowered to 0.5 mV/s

the peak around +0.88V becomes more prominent. The appearance of this peak cannot be explained by the formation of platinum oxides because the oxygen signal in the AES when the electrode is emersed at potentials as high as +0.92V can be attributed to the presence of supporting electrolyte (Figure 10).

Figure 13 shows the deposition from 0.005 mM Ag⁺ onto a clean Pt(111) surface. The scan rate used was again 2.0 mV/s and the initial potential was +0.70V. Similar results were obtained if the starting potential was +0.85V. At this low concentration, there are no discernible peaks related to the deposition of any Ag onto the Pt(111) surface; even the spikes from the clean surface are present in the voltammogram. We continued scanning the potential into the hydrogen region and there is clear evidence for hydrogen adsorption. The amount of free Pt(111) surface calculated from the charge under this region, is $44 \pm 8\%$. It is surprising that with this amount of free Pt surface, the peaks for the removal of the bulk and the second layer of silver are present in the voltammogram. This observation could be explained by three dimensional nucleation of Ag atoms and island formation. These islands will leave bare regions on the Pt(111) surface where hydrogen can be then adsorb. The desorption of the first layer of silver has also two peaks, as in the previous cases, although the current ratio is different. The charge in this region accounts for the removal of about one layer of Ag from the surface (Table 1).

Figure 14 shows a voltammogram similar to the one presented in Figure 13, except the potential was held at +0.15V for 10 minutes. The scan was resumed in the negative direction and hydrogen adsorption was still observed under these conditions. The amount of hydrogen adsorption accounts for $11 \pm 3\%$ of the electrode surface free of deposited Ag. Reversal of the potential in a positive direction shows the stripping of the bulk and the second layer as well as the removal of the first monolayer. These results are consistent with the aforementioned

mechanism. *Thus, it appears that the electrodeposition of Ag^+ on Pt(111) at low concentrations is via nucleation and the formation of islands.*

The voltammetric features associated with removal of the first monolayer are now similar those in 0.10 mM Ag^+ at 0.5 mV/s where the appearance of the peak at +0.88V was evident. The only similarity between the two experiments is the long time interval required to perform both experiments. It may be that the appearance of this peak (+0.88V) is related to a kinetically hindered site on the Pt(111) surface which can be occupied only after a rearrangement of the Ag layer at long times. This is consistent with the fact that the charge under this region is identical for the different experiments regardless of the shape of the peaks.

We have also carried out some studies on the mechanism of electrodeposition of silver from 1.00 and 0.10 mM solutions by depositing a specific amount of Ag onto the surface and removing the excess Ag^+ in solution with pure supporting electrolyte. The potential was then scanned in the negative direction into the hydrogen region to determine the number of bare sites on the Pt surface. Although a detailed account of this process will be given in a future communication, we wish to report a unique and surprising behavior after the deposition of the third peak. Figure 15 shows the cyclic voltammogram for silver deposition from 1.00 mM Ag^+ up to but not including bulk deposition and the associated stripping after rinsing three times with supporting electrolyte at controlled potential. The potential scan was then resumed in the positive direction and the peak for the removal of the second layer of Ag was washed away with the supporting electrolyte. This experiment was also performed by rinsing at open circuit and similar results were obtained. We even deposited Ag^+ on an I/Pt(111) surface to see if iodine, the outermost atom after the deposition, prevented the removal of the second layer, but the results were the same; Ag was removed from the surface. *Thus, extreme care must be taken when the UPD layer is rinsed with*

supporting electrolyte because it can be washed away. This point is also relevant for UHV experiments, where the metal surface is usually rinsed with supporting electrolyte or a dilute solution of the species under study before the transfer to the main chamber to perform electron spectroscopic and/or diffraction experiments.

Figure 16 shows the same experiment as in Figure 15, except this time the concentration of Ag^+ was 0.10 mM. At this concentration, the peak for the second layer was retained on the surface, although the peak was wider than with Ag^+ present in solution. In order to avoid kinetic complications, we performed the same experiment at 0.5 mV/s and similar results were obtained. The reason for the retention of the silver layer at this concentration may be explained by the formation of different structure from that formed at 1.00 mM Ag^+ . Studies for the determination of the surface structure with LEED and X ray diffraction are underway to explore this possibility. For now, we can deduce that the first layer is depositing in a similar way because the stripping of this layer is identical at both silver concentrations after the rinsing experiments.

In summary, we have found that the voltammetry for the deposition of Ag^+ on Pt(111) depends on the Ag^+ concentration used, but it does not follow the Nernstian behavior of 60 mV/decade; only the completion of the second layer follows such behavior. The mechanism for the deposition at low concentrations (<0.01 mM) is via nucleation and island formation, whereas at high concentrations (>1.00 mM) it is in an ordered fashion through the Stranski-Krastanov mechanism. Rinsing the surface with supporting electrolyte after deposition of the second layer results in the removal of this layer when the deposition is from a concentration of 1.00 mM Ag^+ , whereas it is retained when the deposition is from a solution of 0.10 mM Ag^+ . Different surface structures may be responsible for this observation.

ACKNOWLEDGMENTS

This work was supported by the Army Research Office and the Office of Naval Research. JFR acknowledges support by a Ford Foundation Post Doctoral Fellowship. HDA is a A.P. Sloan Foundation Fellow (1987-1991).

REFERENCES

1. G.W. Tindall and S. Bruckenstein, *Electrochim. Acta* 16 (1971) 245-253.
2. S.H. Cadle and S. Bruckenstein, *Anal. Chem.* 43 (1971) 1858-1862.
3. S. Stucki, *J. Electroanal. Chem.* 80 (1977) 375-385.
4. J.S. Hammond and N. Winograd, *J. Electroanal. Chem.* 80 (1977) 123-127.
5. J.L. Stickney, S.D. Rosasco, D. Song, M.P. Soriaga and A.T. Hubbard, *Surf. Sci.* 130 (1983) 326-347.
6. F. El Omar, R. Durand and R. Faure, *J. Electroanal. Chem.* 160 (1984) 385-392.
7. D.G. Frank, T. Golden, F. Lu and A.T. Hubbard, *MRS Bulletin*, 15 (1990) 19-22.
8. R.C. Salvarezza, D. Vázquez Moll, M.C. Giordano and A.J. Arvia, *J. Electroanal. Chem.* 213 (1986) 301-312.
9. D.C. Alonzo and B.R. Scharifker, *J. Electroanal. Chem.* 274 (1989) 167-178.
10. B. Pajarón Costa, J. Canullo, D. Vázquez Moll, R.C. Salvarezza, M.C. Giordano and A.J. Arvia, *J. Electroanal. Chem.* 244 (1988) 261-272.
11. D. Aberdam, C. Salem, R. Durand and R. Faure, *Surface Science* 239 (1990) 71-84.
12. J.E. Harris, M.E. Bothwell, J.F. Rodríguez, M.P. Soriaga and J.L. Stickney, *J. Phys. Chem.* 93 (1989) 2610-2614.
13. D. Kolb in H. Gerisher and C. Tobias (Ed.), *Advances in Electrochemistry and Electrochemical Engineering*, Vol. 11, J. Wiley and Sons, New York, 1978, p. 125.
14. R.R. Adzic in H. Gerisher and C. Tobias (Ed.), *Advances in Electrochemistry and Electrochemical Engineering*, Vol. 13, J. Wiley and Sons, New York, 1987, p. 161.
15. J.H. White and H.D. Abruña, *J. Phys. Chem.* 94 (1990) 894.
16. J. Clavilier, *J. Electroanal. Chem.* 107 (1980) 211.
17. D. Aberdam, R. Durand, R. Faure, F. El-Omar, *Surf. Sci.* 171 (1986) 303.
18. D.F. Untereker, W.G. Sherwood and S. Bruckenstein, *J. Electrochem. Soc.* 125 (1978) 380.
19. F.T. Wagner and P.N. Ross, *J. Electroanal. Chem.* 150 (1983) 141.

20. M.T. Paffett, C.T. Campbell and T.N. Taylor, *Langmuir* 1 (1985) 741-747.
21. P.W. Davies, M.A. Quinlan, G.A.Somorjai, *Surface Science* 121 (1982) 290-342.

FIGURE CAPTIONS

Figure 1. Auger electron spectrum and LEED pattern for a clean Pt(111) electrode surface. Experimental parameters: AES – Emission current = 0.6 mA, Beam current = 15 μ A, Modulation amplitude = 8 eV, Scan rate = 5 eV/s. LEED – Emission current = 0.2 mA, Beam current = 1 μ A, Screen voltage = 2 kV, Beam voltage = 60 eV.

Figure 2. Cyclic voltammogram for clean Pt(111) using the flame annealing procedure as pre-treatment. Experimental parameters: Scan rate 50 mV/s, Area = 0.71 cm².

Figure 3. Ultra-high vacuum chamber which contains instrumentation to perform electrochemical and surface characterization studies.

Figure 4. Cyclic voltammogram for a clean Pt(111) electrode pre-treated in the UHV. Experimental parameters; Scan rate = 2.0 mV/s, Area = 0.50 cm².

Figure 5. AES and LEED pattern for clean Pt(111) after cyclic voltammetry in 0.10 M H₂SO₄. The electrode was emersed at +0.40V. Other experimental parameters are the same as in Figure 1.

Figure 6. Electrochemical cell used to perform experiments outside the UHV.

Figure 7. Deposition of silver from 1.00 mM on two different pre-treated Pt(111) surfaces in 0.10 M H₂SO₄ starting from +0.85V. A – The electrode was cleaned and characterized in the UHV with AES and LEED. B – The electrode was flame annealed to obtain the long range order of the surface. Experimental parameters: A – SR = 2.0 mV/s, A = 0.50 cm²; B – SR = 2.0 mV/s, A = 0.71 cm².

Figure 8. Cyclic voltammogram for clean Pt(111) starting at +0.85V. Experimental parameters: SR = 2.0 mV/s, A = 0.71 cm².

Figure 9. LEED pattern after deposit one layer of Ag from a 1.00 mM solution. Experimental parameters are the same as in Figure 1.

Figure 10. Auger electron spectrum after emersion at +0.92V from 1.00 mM Ag⁺/0.10 M H₂SO₄. Experimental parameters are the same as in Figure 1.

Figure 11. Deposition of silver from a 0.10 mM solution on a Pt(111) surface in 0.10 M H₂SO₄ starting from +0.85V. Experimental parameters are the same as in Figure 7B.

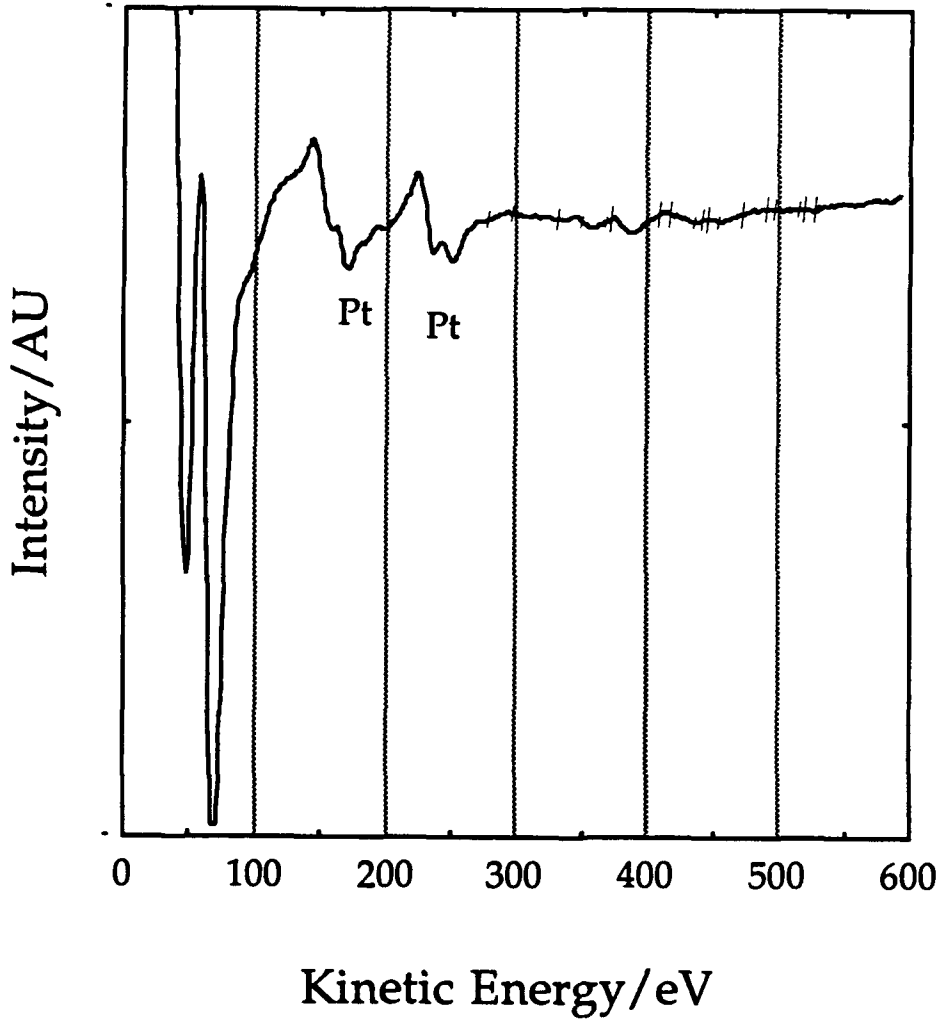
Figure 12. Deposition of silver from a 0.10 mM solution on a Pt (111) electrode surface at a scan rate of 0.5 mV/s. Other experimental parameters are the same as in Figure 7B.

Figure 13. Deposition from 0.005 mM Ag⁺ on a Pt(111) surface in 0.10 M H₂SO₄ starting from +0.70V. Experimental parameters are the same as in Figure 7B.

Figure 14. Deposition from 0.005 mM Ag⁺ on a Pt(111) surface in 0.10 M H₂SO₄ starting from +0.70V and holding the potential at +0.15V for 10 minutes. Experimental parameters are the same as in Figure 7B.

Figure 15. Deposition of two Ag layers from 1.00 mM solution. The potential was held at +0.36V until an equilibrium was reached. The electrode was rinsed three times with 0.10 M H₂SO₄ at controlled potential. The scan was resumed in the positive direction after rinsing. Experimental parameters are the same as in Figure 7B.

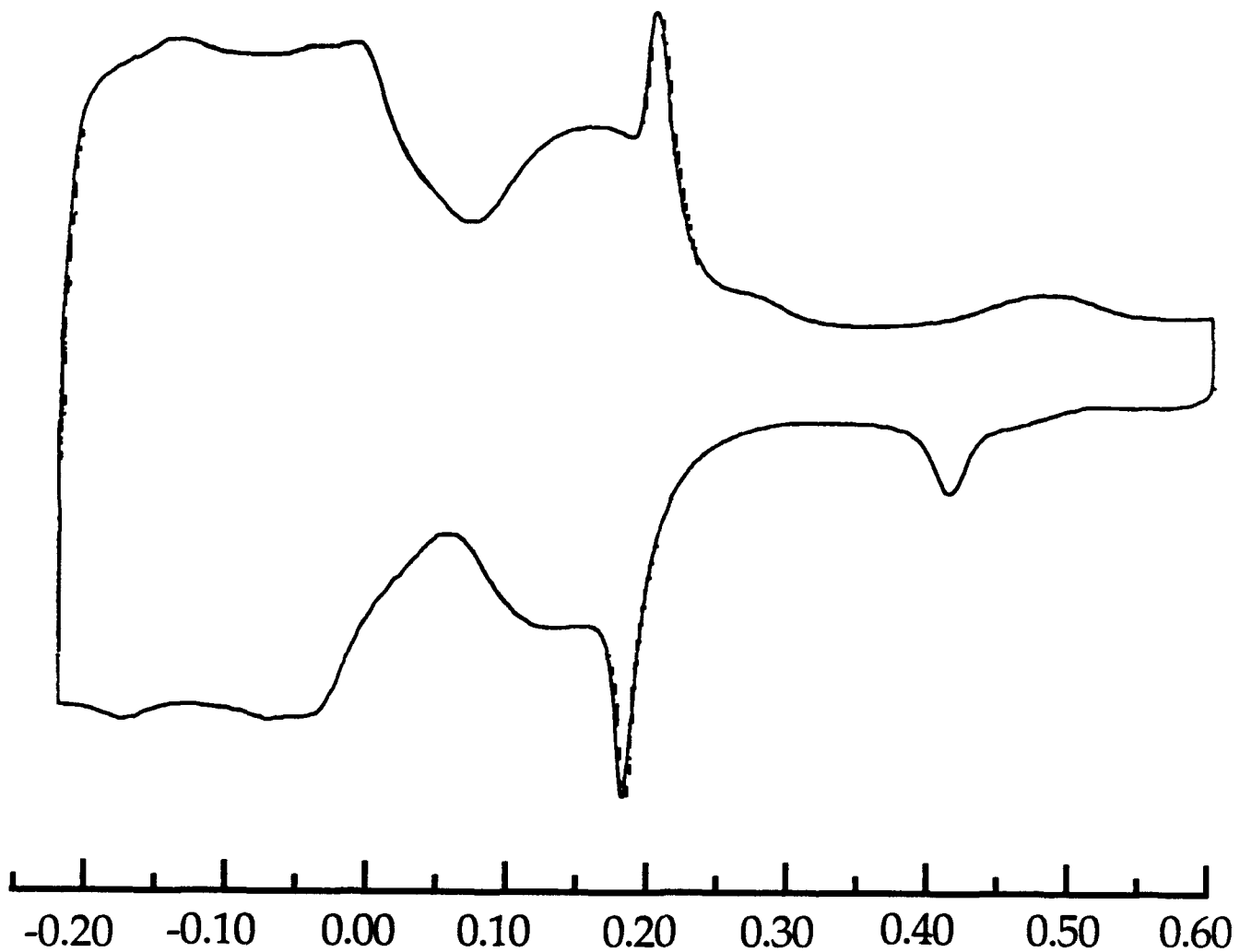
Figure 16. Deposition of two Ag layers from 0.10 mM solution and the potential was held at +0.27V until an equilibrium was reached. The electrode was rinsed three times with 0.10 M H₂SO₄ at controlled potential. The scan was resumed in the positive direction after rinsing. Experimental parameters are the same as in Figure 7B.





0.10 M H_2SO_4
50 mV/sec

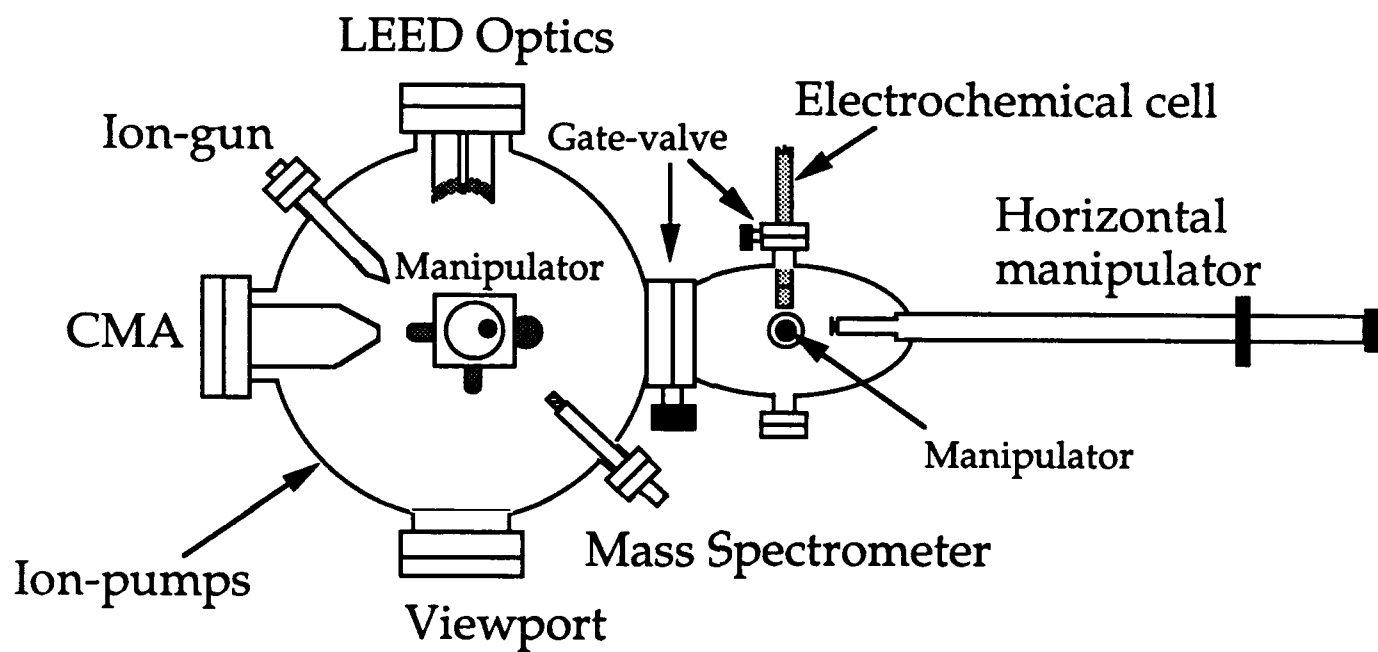
10 μA



E/V vs Ag/AgCl (1M NaCl)

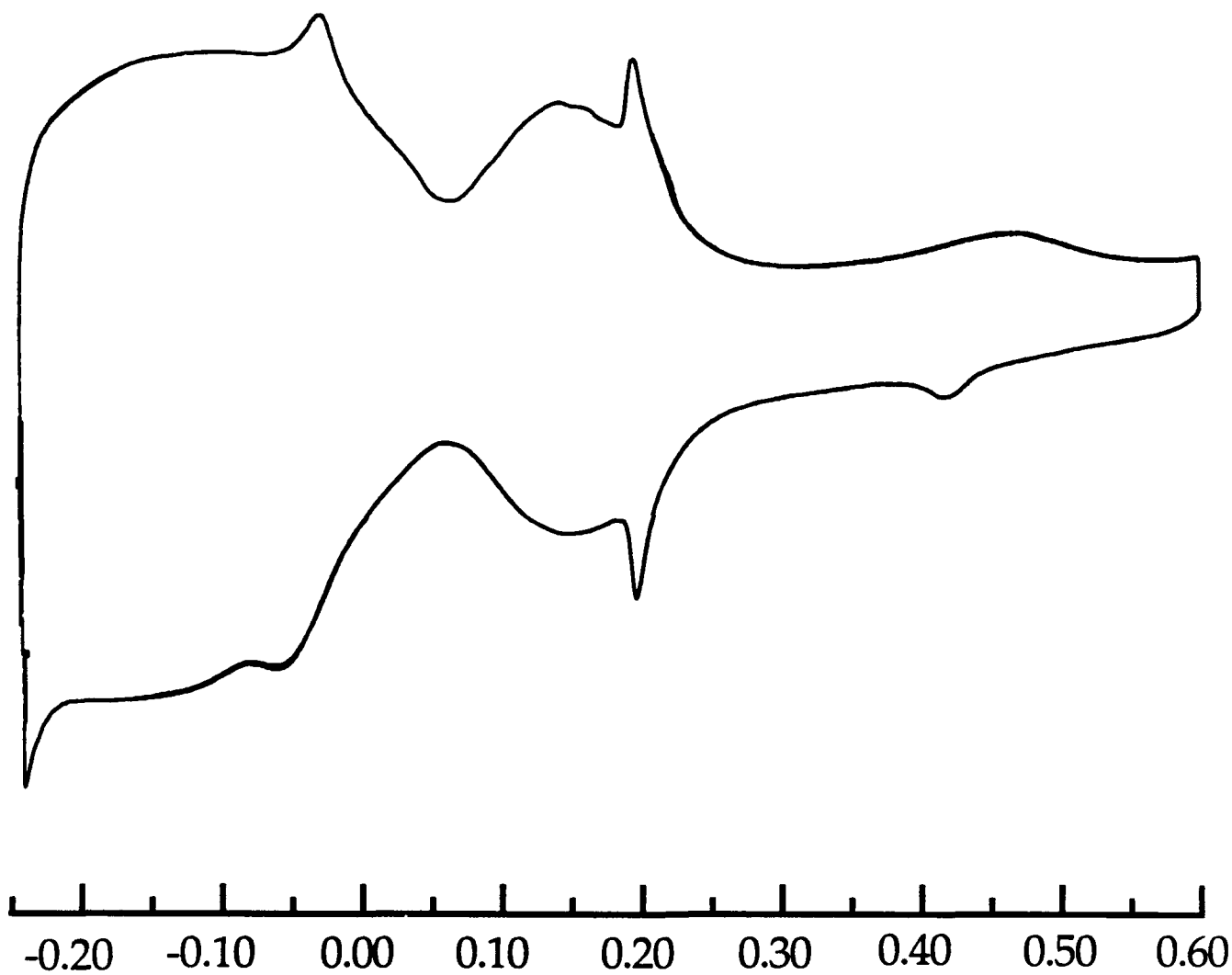
Main chamber

Ante-chamber

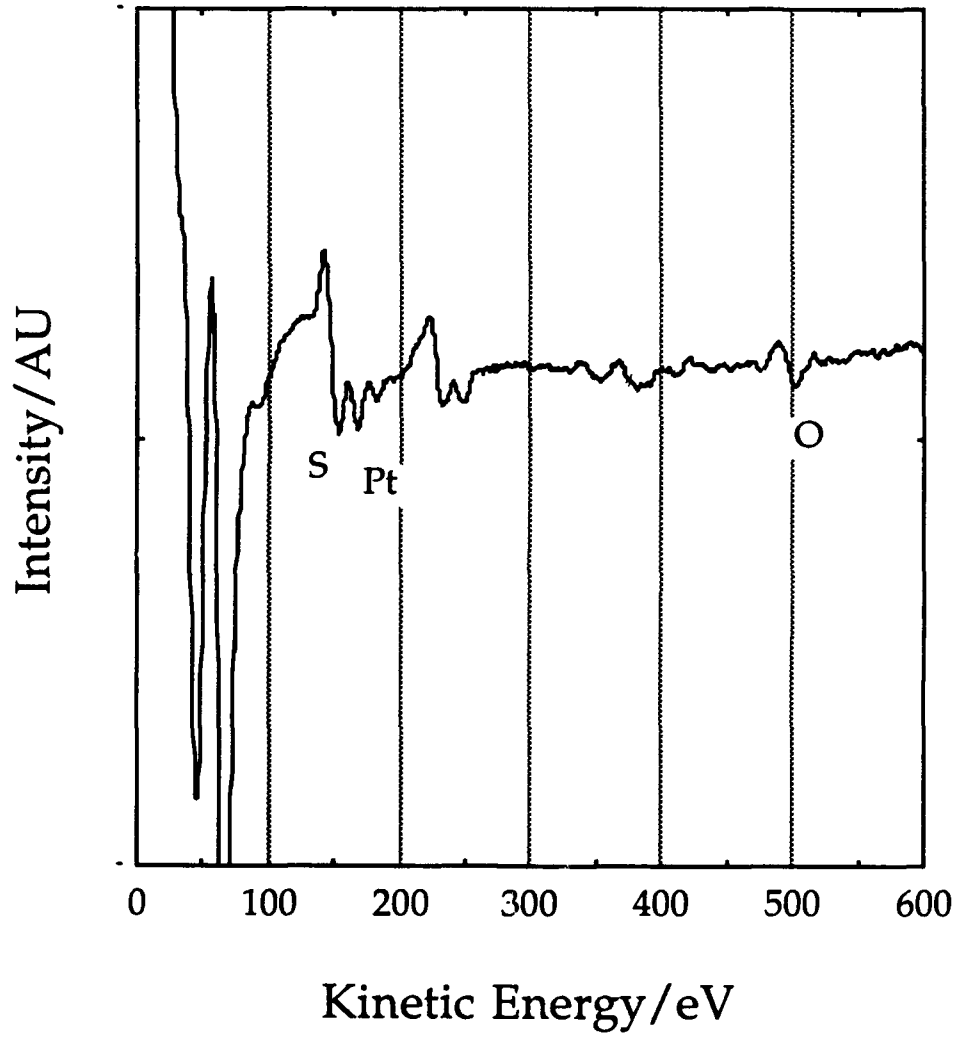


0.10 M H_2SO_4
50 mV/sec

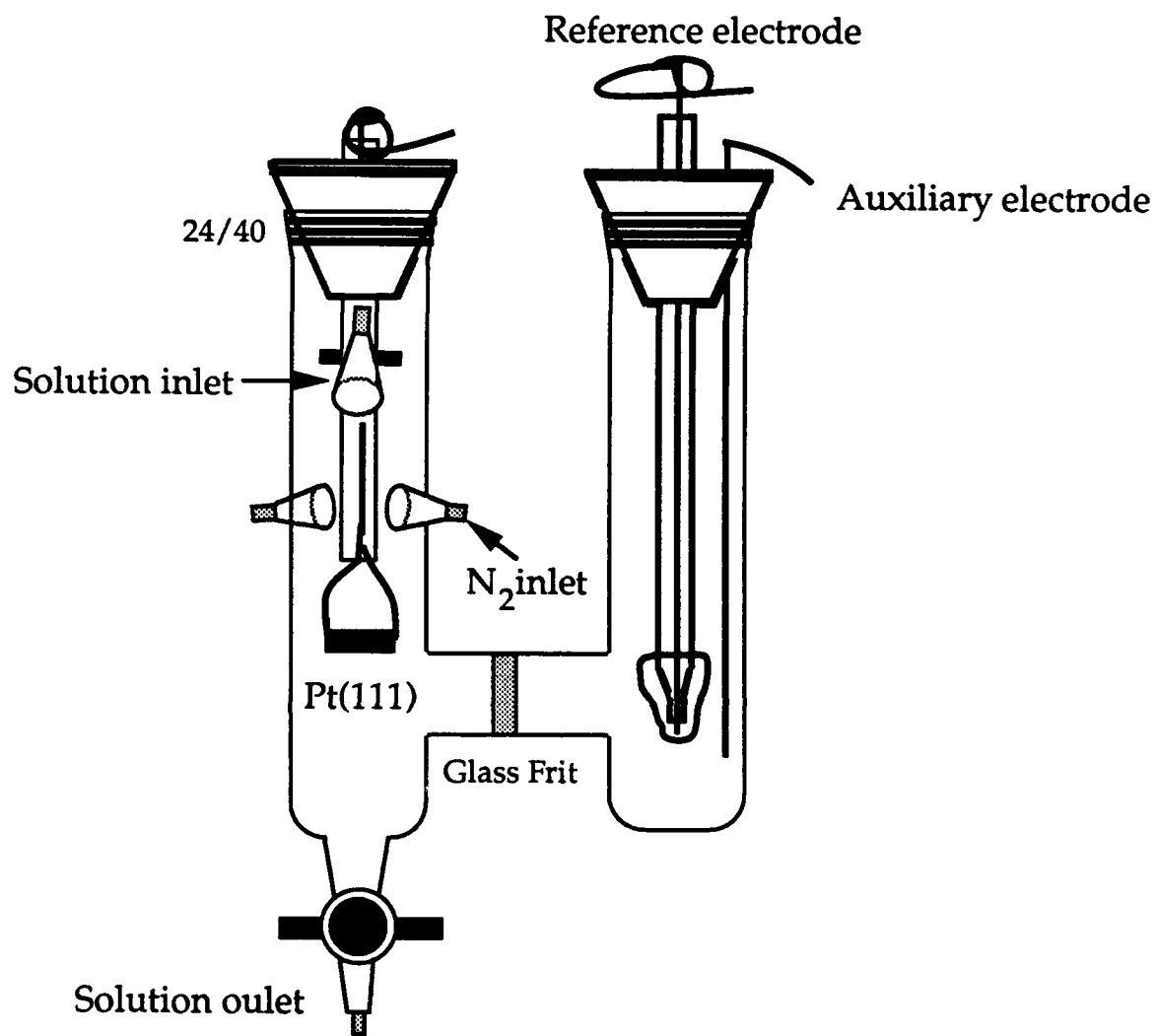
10 μA



E/V vs Ag/AgCl (1M NaCl)



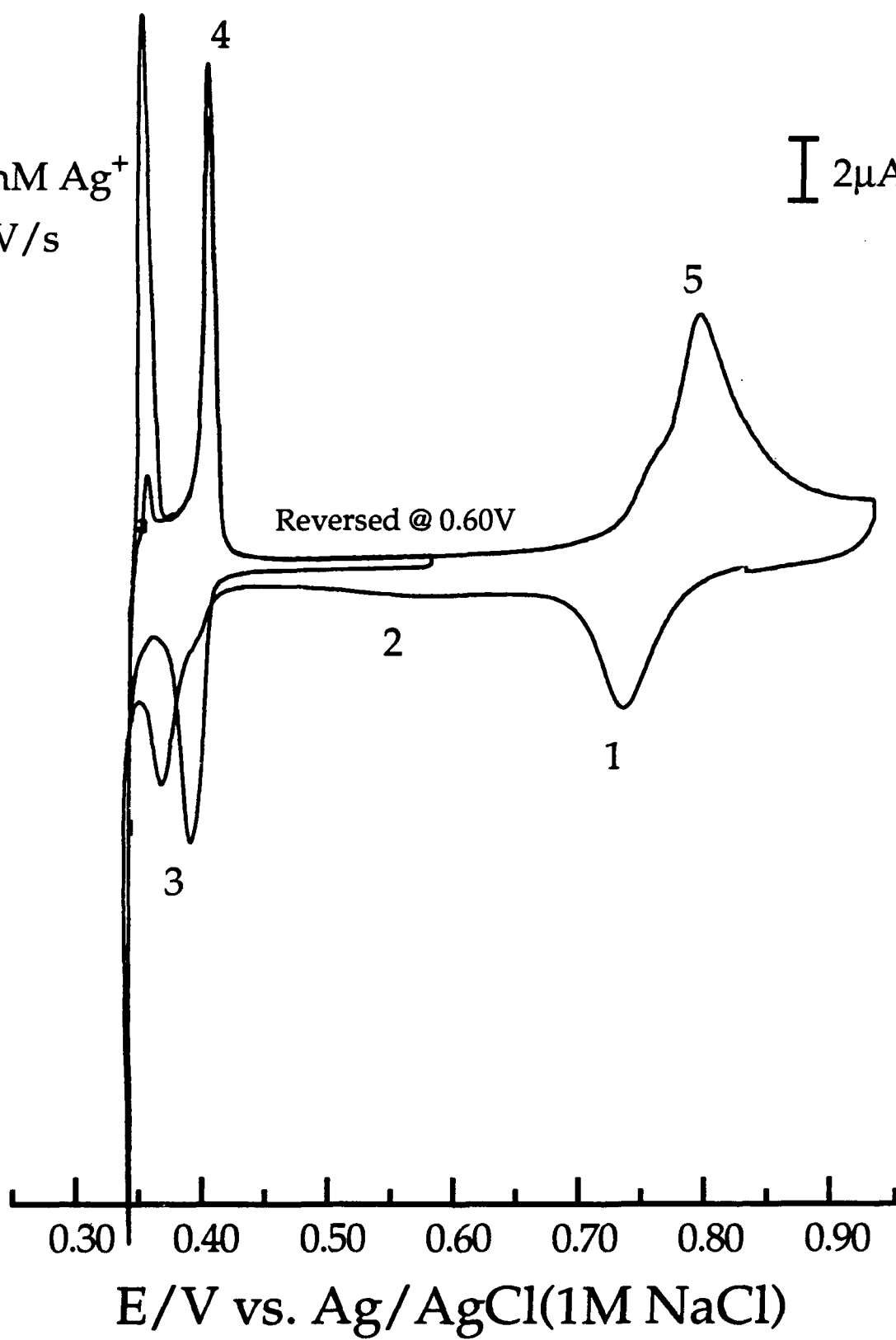




A

1.00 mM Ag^+
2.0 mV/s

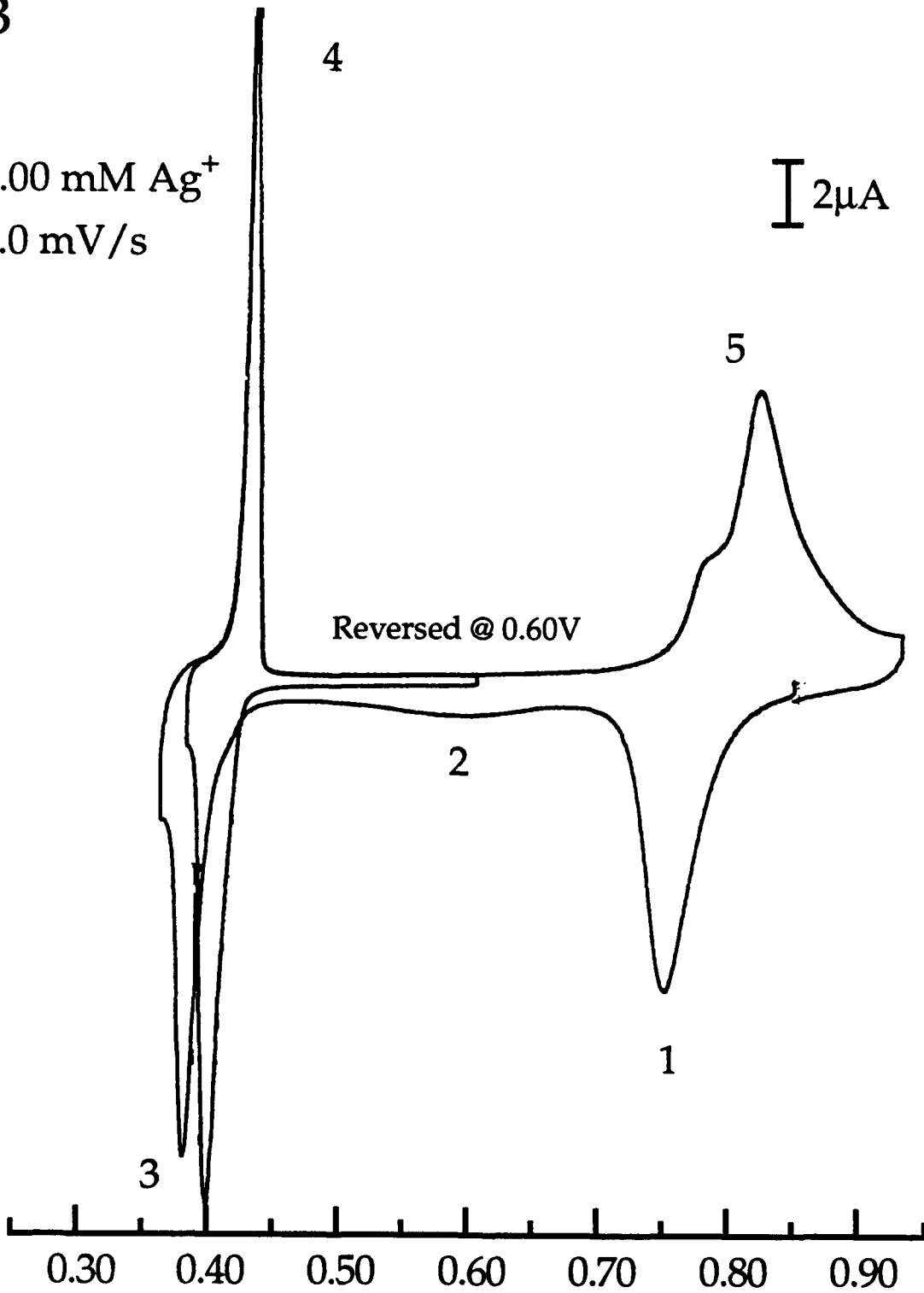
I 2 μA



B

1.00 mM Ag^+
2.0 mV/s

I 2 μA

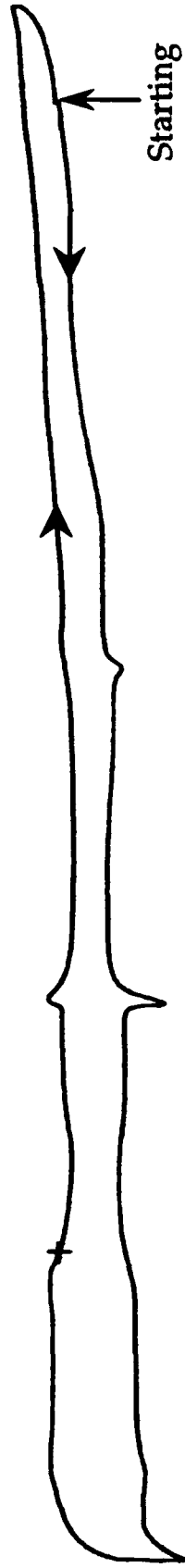


E/V vs. Ag/AgCl(1M NaCl)

0.10 M H_2SO_4

2.0 mV/s

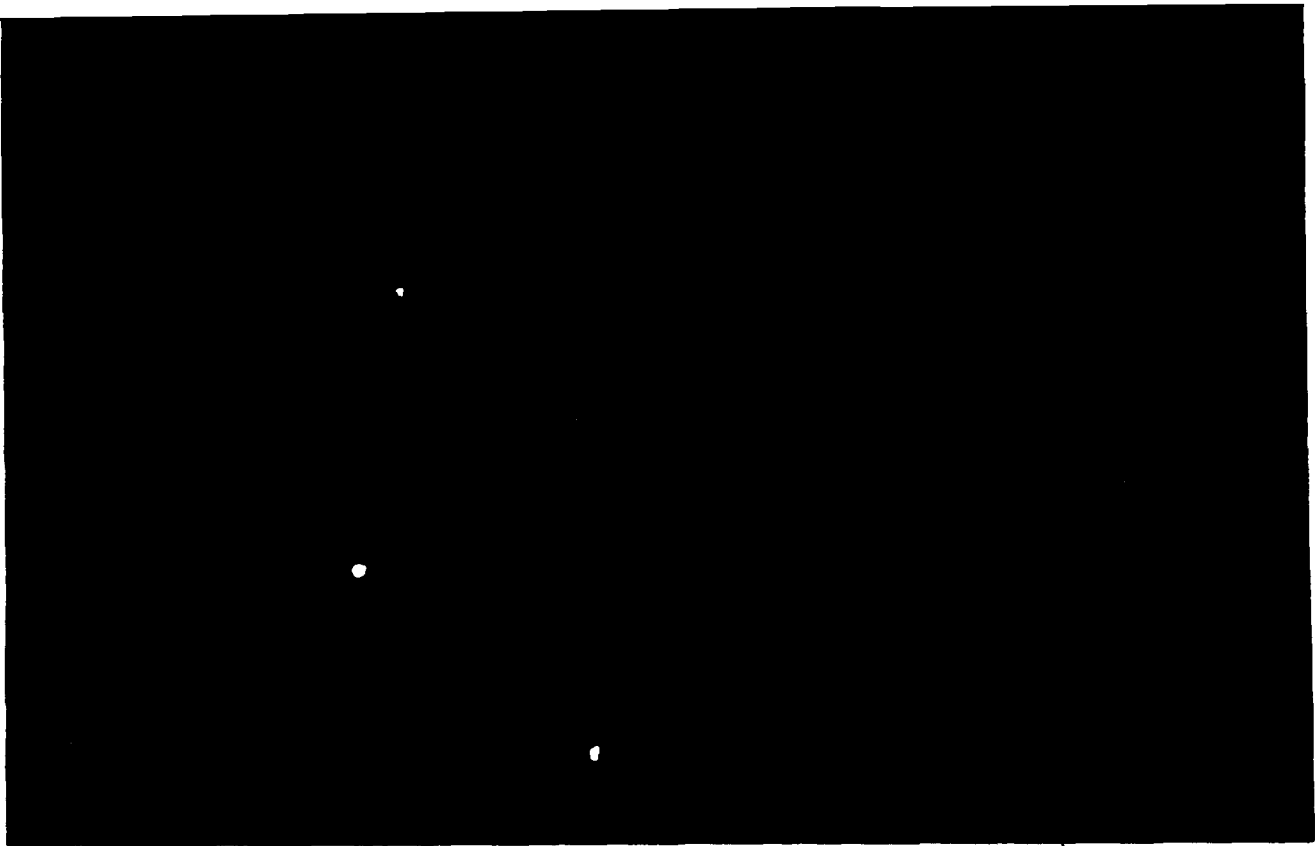
I 2 μA



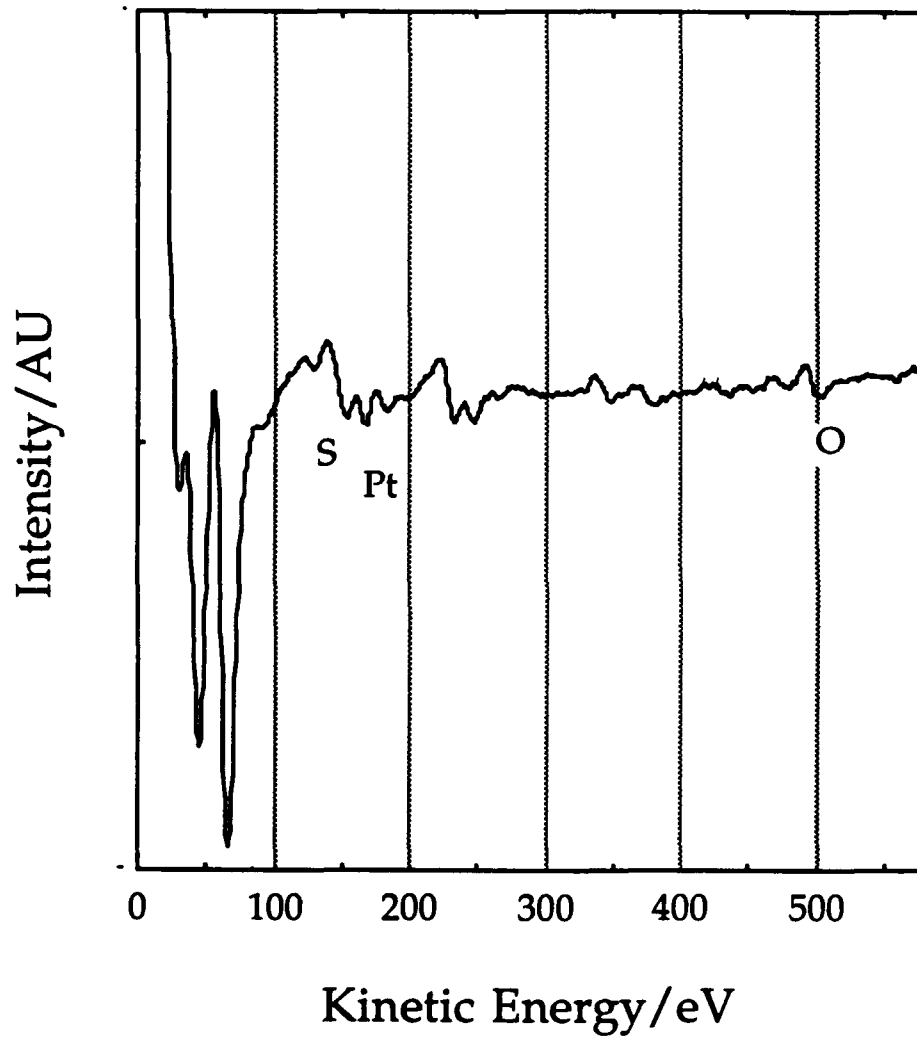
Starting
Potential

-0.25 -0.15 -0.05 0.05 0.15 0.25 0.35 0.45 0.55 0.65 0.75 0.85 0.95

E/V vs. AgCl(1M NaCl)



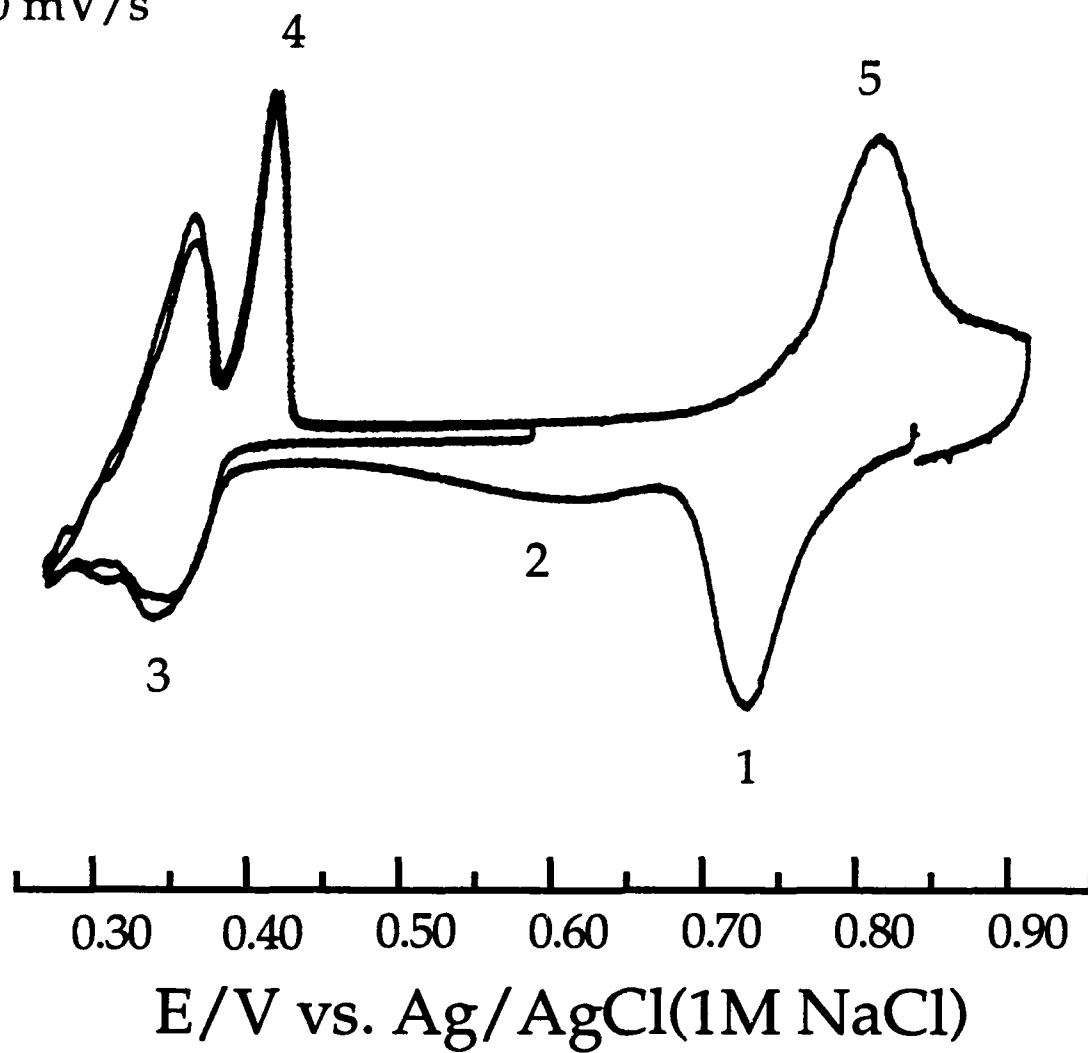
11
12

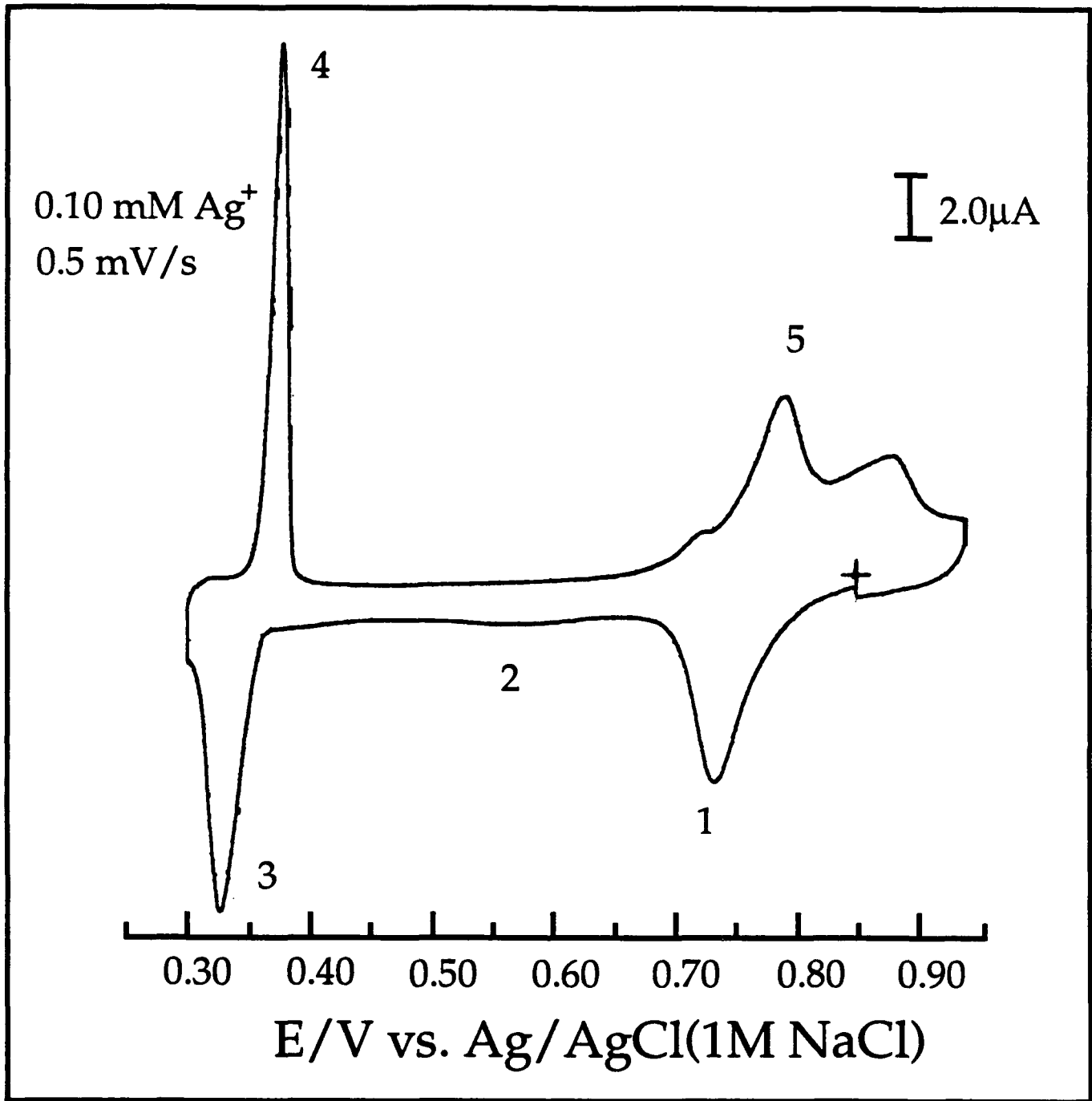


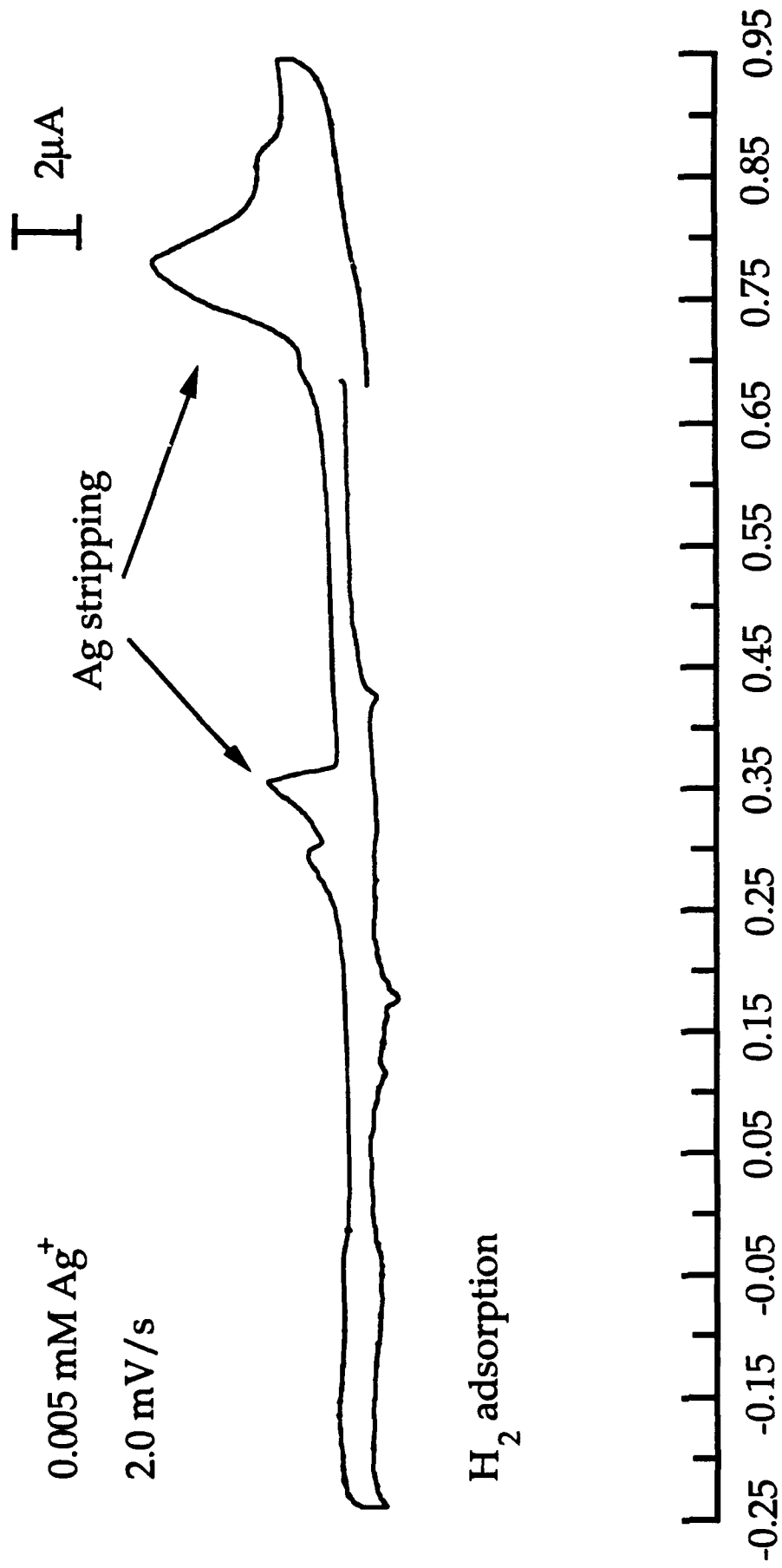
0.10 mM Ag⁺

2.0 mV/s

2.0 μA





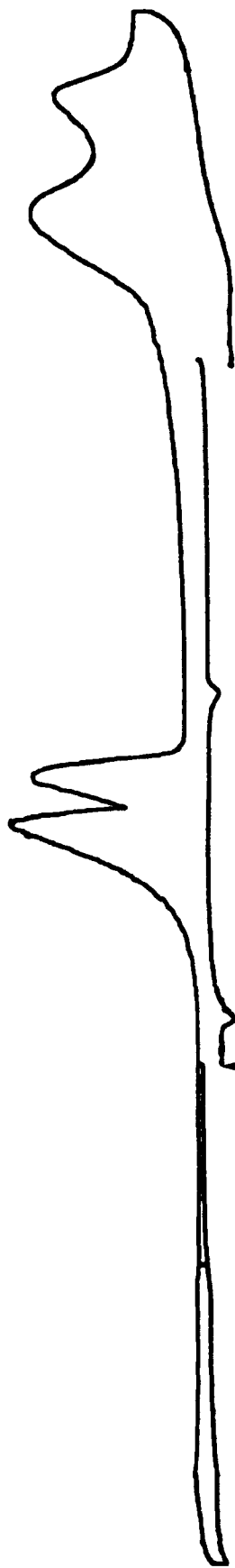


0.005 mM Ag^+

2.0 mV/s

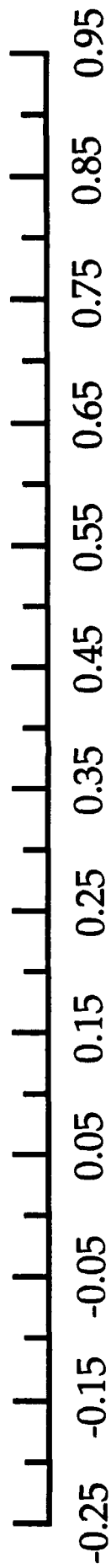
I 2 μA

Ag stripping



H₂ adsorption

Hold for
10 min.

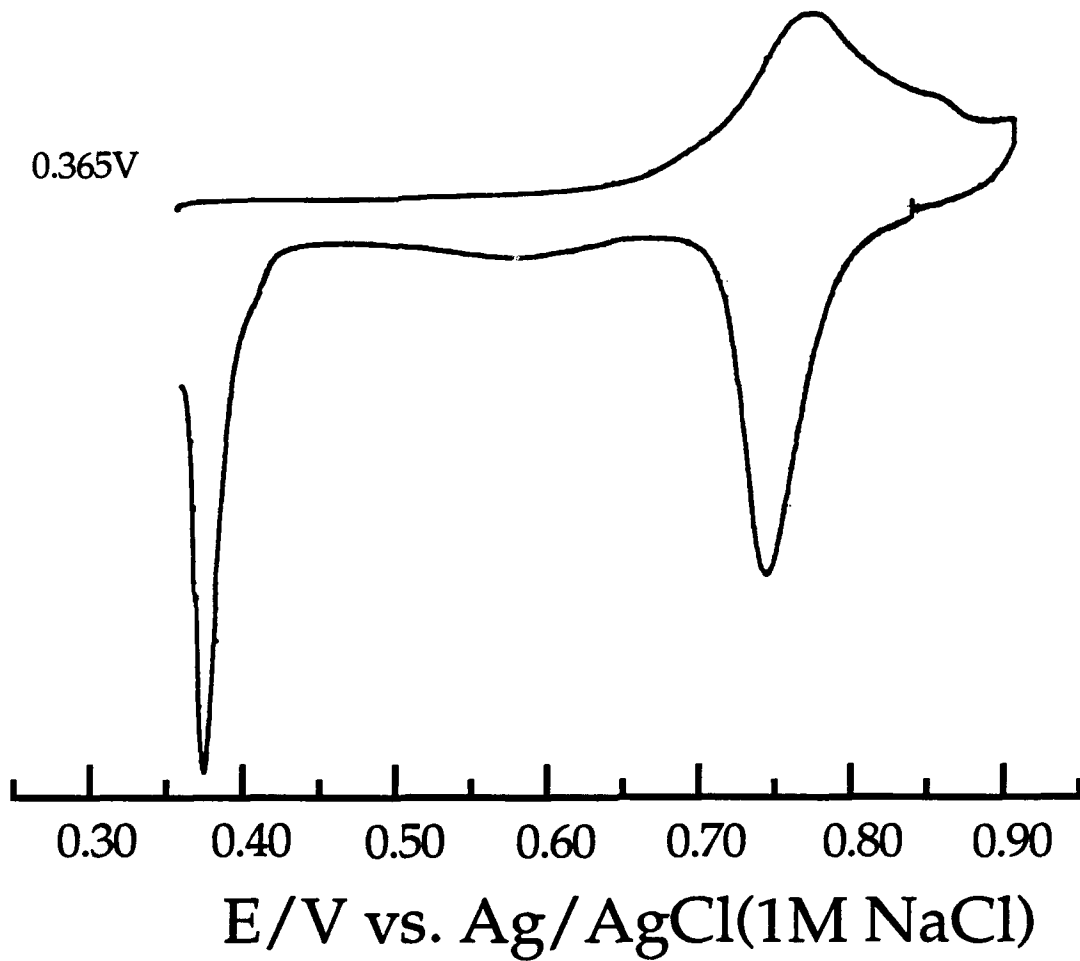


E/V vs. Ag/AgCl(1M NaCl)

1.00 mM Ag⁺

2.0 mV/s

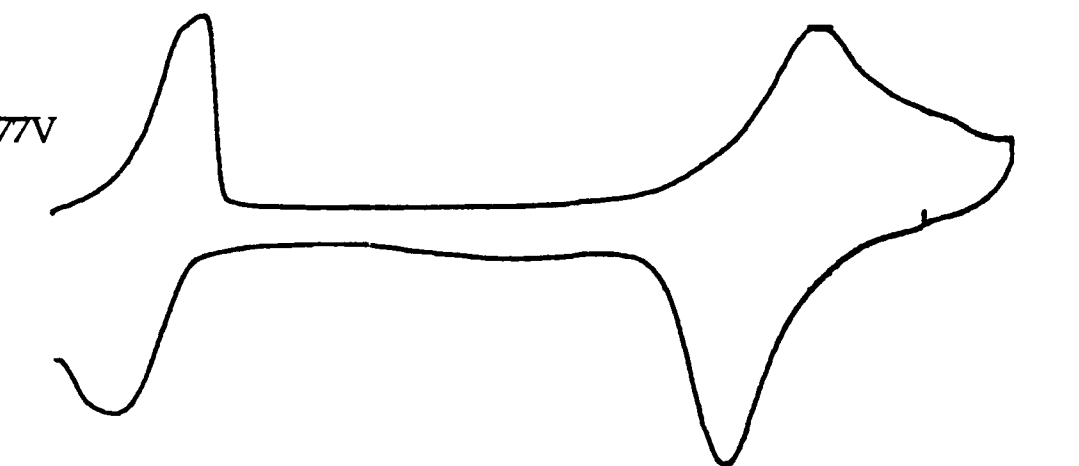
I 2.0 μA



1.00 mM Ag⁺
2.0 mV/s

2.0 μA

0.277V



0.30 0.40 0.50 0.60 0.70 0.80 0.90

E/V vs. Ag/AgCl(1M NaCl)

Table 1. Charge and surface coverage of silver in various potential regions.

1.00 mM Ag⁺(2 mV/s)	Charge/μC	Surface coverage/nmoles cm⁻²
Peak 1 (0.85-0.69)V	300 \pm 15	1.30 \pm 0.09
Peak 2 (0.69-0.45)V	49 \pm 6	0.22 \pm 0.03
Peak 3 (0.45-0.36)V	180 \pm 15	0.81 \pm 0.09
Peak 4 (0.39-0.45)V	162 \pm 15	0.75 \pm 0.09
Peak 5 (0.70-0.92)V	370 \pm 20	1.66 \pm 0.09

0.10 mM Ag⁺(2 mV/s)	Charge/μC	Surface coverage/nmoles cm⁻²
Peak 1 (0.85-0.69)V	290 \pm 15	1.30 \pm 0.09
Peak 2 (0.69-0.45)V	36 \pm 6	0.16 \pm 0.03
Peak 3 (0.45-0.36)V	128 \pm 15	0.54 \pm 0.09
Peak 4 (0.39-0.45)V	180 \pm 15	0.81 \pm 0.09
Peak 5 (0.70-0.92)V	352 \pm 20	1.58 \pm 0.09

0.10 mM Ag⁺(0.5 mV/s)	Charge/μC	Surface coverage/nmoles cm⁻²
Peak 1 (0.85-0.69)V	238 \pm 15	1.07 \pm 0.09
Peak 2 (0.69-0.45)V	45 \pm 6	0.20 \pm 0.03
Peak 3 (0.45-0.36)V	178 \pm 15	0.81 \pm 0.09
Peak 4 (0.39-0.45)V	200 \pm 15	0.90 \pm 0.09
Peak 5 (0.70-0.92)V	381 \pm 20	1.70 \pm 0.09

Cont. Table 1

0.005 mM Ag⁺(0.5 mV/s)	Charge/μC	Surface coverage/nmoles cm⁻²
Bulk and Second Layer	86 \pm 12	0.38 \pm 0.08
Peak 5 (0.70-0.92)V	313 \pm 20	1.40 \pm 0.09
Hydrogen region	224 \pm 20	44 \pm 5%*

0.005 mM Ag⁺(0.5 mV/s) (Hold @ 0.15V/10 min.)	Charge/μC	Surface coverage/nmoles cm⁻²
Bulk and Second Layer	264 \pm 12	1.18 \pm 0.08
Peak 5 (0.70-0.92)V	322 \pm 20	1.40 \pm 0.09
Hydrogen region	87 \pm 12	11 \pm 5%*

* The surface coverage for this case is the percentage calculated from the ratio for the Ag⁺ deposition and the clean surface from the hydrogen region starting from +0.05V.

Table 2. Differences in the peak positions for silver deposition from 0.10mM and 1.00mM concentrations.

Peak number	0.10mM Ag⁺(E/mV)	1.00mM Ag⁺(E/mV)	Difference(E/mV)
1	717	742	25
2	570	580	10
3	321	374	53
4	409	438	29
5	810	823	13